XMM-NEWTON OBSERVATIONS OF LUMINOUS NARROW-LINE SEYFERT 1 GALAXIES

Chiho Matsumoto[1], **Karen M. Leighly**[2], **and Toshihiro Kawaguchi**[3]

[1]EcoTopia Science Institute, Nagoya University, Furo-cho, Chikusa, Nagoya, 464-8603, Japan
[2]Department of Physics and Astronomy, The University of Oklahoma, 440 West Brooks St., Norman, OK 73019
[3]Optical and Infrared Astronomy Division, National Astronomical Observatory of Japan, Osawa 2-21-1, Mitaka, Tokyo 181-8588, Japan

ABSTRACT

We present results from the XMM-Newton observations of four optically-luminous narrow-line Seyfert 1 galaxies. The obtained X-ray spectra showed that intrinsic absorption is unlikely to be present; all the four X-ray spectra are steep, as is typical among narrow-line Seyferts. Utilizing simultaneous UV observations by the OM, we also investigate the spectral energy distributions in the UV–X-ray band. One object (RX J1225.7+2055) of the four was found to be X-ray weak (the spectral energy index between 2500 Å and 2 keV: $\alpha_{\rm ox}\sim$2.0) during our observations. Compiling values of $\alpha_{\rm ox}$ from a larger sample of narrow-line Seyferts, we find that, although the sample is small, the $\alpha_{\rm ox}$ distribution suggests that X-ray weakness may occur more frequently among more luminous objects. This suggest that X-ray weakness may be caused by high accretion rate. We try to interpret the $\alpha_{\rm ox}$ dependence on the optical luminosity, based on simple disk models of an accretion disk sandwiched by coronae.

Key words: X-rays; Narrow-line Seyfert 1 Galaxies.

1. INTRODUCTION

The extreme spectral and variability properties of narrow-line Seyfert 1 galaxies (NLS1s) have been the subject of intensive study by virtually every X-ray satellite during the past decade, and are now well established. They frequently show a strong soft excess component, their hard X-ray spectrum tends to be steeper than in similar broad-line Seyfert 1 galaxies, and they show rapid and large-amplitude X-ray variability (e.g. Boller et al. 1996; Leighly 1999). NLS1s, defined by their optical emission-line properties: FWHM Hβ $<$ 2000 km s^{-1} and [O III]λ5007/Hβ $<$ 3 (Osterbrock & Pogge 1985; Goodrich 1989), are different from type 2 Seyfert galaxies, which generally have [O III]/Hβ $>$ 3. NLS1s usually have strong permitted lines of Fe II from broad-line region (BLR), which also discriminate NLS1s from type 2 Seyfert galaxies. The most promising explanation for these X-ray and optical properties is that NLS1s have a higher mass accretion rate compared with the Eddington value.

Luminous AGNs with narrow emission lines are of special interest, because they should have particularly high accretion rates based on the reverberation mapping argument (e.g., Laor 2000). If the motion of the BLR gas is dominated by gravity of the central black hole (BH), the velocity dispersion (Δv) is expressed by $\Delta v^2 \simeq GM_{\rm BH}/R_{\rm BLR}$, where $R_{\rm BLR}$ is the radius of the emission line in question. The BLR size is expected to be set by the bolometric luminosity (L), specifically $R_{\rm BLR} = 0.1\left(\frac{L}{10^{46}{\rm ergs\ s^{-1}}}\right)^{0.5}$ pc and this is experimentally verified in reverberation mapping (Kaspi et al. 2000, though with somewhat steeper slope of $\sim$0.7). Combining these two equations reveals $L/L_{\rm Edd} \propto \Delta v^{-2} L^{0.5}$. Therefore, study of luminous NLS1s is particularly important, as it allows examination of the physics under conditions of extremely high $L/L_{\rm Edd}$.

Our study on luminous NLS1s is also inspired by PHL 1811, a quite luminuos ($M_{\rm v} = -26.5$) quasar discovered in the VLA FIRST radio survey. It is extremely bright and optically classified as a NLS1. This object is remarkable because was not a known X-ray source, being undetected in the *ROSAT* all-sky survey (RASS; Voges et al. 1999), nevertheless its brightness (m=13.7). Followup *BeppoSAX* observations detected the quasar in the X-rays, but discovered that it is remarkably X-ray weak (Leighly et al. 2001a). During followup *Chandra* observations in 2001, it was again observed to be X-ray weak. Significant variability was observed between the two observations separated by 12 days, and an observed steep X-ray spectrum shows that it is not absorbed (Leighly et al. 2004; Leighly et al. in prep.). The UV emission line property observed with the *HST* STIS is unusual in that the spectrum is dominated by Fe II and there is no prominent broad emission line; it is consistent with weak X-ray emission(Leighly et al. 2004; Leighly et al. in prep.). These observations argues that PHL 1811 is intrinsically

X-ray weak. Still it is not clear whether or not intrinsic X-ray weakness is common among luminous NLS1s.

In order to begin to generalize the properties of luminous NLS1s (narrow-line quasars, hereafter NLQSOs), we proposed to observe handful NLQSOs with luminosity of $M_{\rm v} < -25$, and four of them are approved and observed (Table 1).

Throughout this paper, uncertainties quoted in the body and tables are 90 % confidence for one parameter of interest.

2. THE *XMM-NEWTON* OBSERVATIONS

We carried out *XMM-Newton* observations of four NLQSOs with scheduled duration of 12 ks for each in 2003. The observation date and fundamental informations of the sources are summarized in Table 1. The EPIC instruments were operated in Full-frame mode for all observations. We used medium filter for most observations; only for the MOS instrument in the RX J2241.8−4405 observation, thick filter is used to suppress events from bright star in the F.O.V. With the optical monitor onboarded *XMM-Newton*, we also scheduled UV photometry with two filters. The RGS was also operated, however, these objects are too faint to investigate with the RGS. We also performed UV photometric observation by the optical monitor (OM; Mason et al. 2001) with two filters for each object. Details of the UV observations are described later in §3.2.

We analyzed pipeline processed products using SAS 5.4.1 and HEAsoft 5.2 and 5.3 packages. We selected only the events with "flag=0" and "pattern=0–4 (pn) or 0–12 (MOS)".

Unfortunately, most of observations happened to be done in the period with quite high background rate. We discarded such data using the method described in the *XMM-Newton* SAS users' guide: First we extracted light curves of the "pattern=0" events with the energy greater than 10 keV, and the quiet background period was defined when the count rate was lower than the recommended values of 0.35 c s^{-1} and 1.0 c s^{-1} for the MOS and the pn, respectively. For most instruments, "good" exposures are 30–70 % of the total pipeline processed durations. The length is summarized in Table 1. In the worst case of the pn observation of RX J2241.8−4405, no good exposure is obtained with the above criterion. If we increased the threshold five times higher than the users' guide value, exposure of 0.6 ks is selected. We used this pn data of RX J2241.8−4405 only for the purpose to check whether the MOS results is consistent with that.

The sources are clearly seen at the positions which are consistent with the optical positions. We made plots of the point spread function (radial profile of the count rate) of the sources; The plots show no signature of spatial extension for all sources, and also show that photons from the source are dominating background photons at radii smaller than several ten arcseconds even for the faintest source. Thus, the source photons are collected from the region of $r < 35''$ for all. The background photons are collected from the near region avoiding serendipitous sources.

To look at variability, we extracted "cleaned" X-ray light curves in the 0.3–10 keV band. The fit to each light curve with a constant model is not rejected, hence, significant short-term variability is not detected during our observations. This is not surprising because our observations were pretty short in duration, and because the photon-statistics are not so great. The light curve with the highest photon-statistics from PG 2233+134 suggests marginal variability with time-scale of ∼1000 s.

3. ANALYSES & RESULTS

3.1. X-ray Spectra

The extracted pn and MOS spectra are grouped so that each energy bin has 20 photons at least; then, we used χ^2 fitting method. The detector response matrices were created by rmfgen and arfgen in SAS.

First, we fitted each spectrum in the whole energy band (0.3–10 keV) with a model of a power law attenuated by Galactic absorption. After confirming that the results from each detector are consistent among them, we fitted the pn and MOS spectra simultaneously[1] with the same model. For RX J2241.8−4405 and PG 2233+134, this model was rejected at 90 % confidence level. We also made fits with the same model only in the 2–10 keV band, this fit was acceptable for every target. The obtained power-law indices from both fits are summarized in Table 1. The results shows that all the X-ray spectra are pretty steep with $\Gamma > 2$, as is typical among NLS1s (e.g. Pounds et al. 1995; Boller et al. 1996; Brandt et al. 1997; Leighly 1999).

The observed steep X-ray spectra strongly implies no significant intrinsic absorption. If there is absorption material with $N_{\rm H}$ of 10^{21-24} $\rm cm^{-2}$, the EPIC spectrum should have convex curvature; but it is not observed. One possibility remains not to be rejected, where the absorption column is quite large ($N_{\rm H} \gtrsim 10^{25}$ $\rm cm^{-2}$) and the observed X-rays are not direct emission from the nucleus but the scattered light, as sometimes seen in Seyfert 2 galaxies. In this case, neutral-iron K-emission line with an huge equivalent width (EW) of larger than 1 keV is considered to be accompanied (e.g., Ghisellini, Haardt, & Matt, 1994). The obtained spectra yielded that the upper-limit of a narrow iron-line EW is 0.7, 0.2, 0.8, and 6 keV for RX J2241.8−4405, PG 2233+134, PG 1543+489, and RX J1225.7+2055, respectively. Thus, we can say that

[1]The pn data is not used in the analyses of RX J2241.8−4405, as mentioned before.

Table 1. Results from the XMM-Newton *observations of luminous NLS1s.*

Object Name	z	M_v	m	N_H^a	Obs. Date Time	$\Gamma_{0.3-10keV}$	$\Gamma_{2-10keV}$	$F^a_{2-10keV}$	α_{ox}
RX J2241.8−4405	0.545	−26.9	15.8	1.8	5/28 15–18(UT)	$(2.64\pm0.10)^b$	2.4±0.4	4.2×10^{-13}	1.52
PG 1543+489	0.400	−25.6	16.0	1.6	2/08 20–24(UT)	2.74±0.07	2.6±0.5	1.5×10^{-13}	1.58
PG 2233+134	0.325	−25.2	16.0	4.8	5/17 17–20(UT)	$(2.56\pm0.04)^b$	2.2±0.2	5.4×10^{-13}	1.54
RX J1225.7+2055	0.335	−25.1	15.9	2.4	6/12 16–20(UT)	$2.73^{+0.29}_{-0.25}$	...	0.2×10^{-13}	1.95

a: The unit of Galactic column density is 10^{20} cm^{-2}, and that of the 2–10 keV flux is erg cm^{-2} s^{-1}.
b: The χ^2 value of this fit was unacceptable at 90 % confidence level, and the fit was improved significantly by the addition of a soft excess component.

all but RX J1225.7+2055, at least, are not attenuated by heavy absorption based on the iron-line upper limit.

For RX J2241.8−4405, an iron-emission-line is marginally detected at the central energy of 6.7±0.3 keV with the EW of 300^{+365}_{-260} eV; however, because the detection is just based on a single energy bin in the MOS spectrum, this validity should be examined by further observation.

Soft excess component is another common spectral feature among NLS1s; Actually, its existence is implied for some sources in the ratio plots of the data to the extrapolated best-fit power-law model in the 2–10 keV band. As a trial, we fitted the 0.3–10 keV spectra with the power-law plus a blackbody model. By adding a blackbody component, the fits are improved significantly (>99% by F-test) for RX J2241.8−4405 and PG 2233+134. The blackbody temperatures are obtained to be 0.14±0.02 keV and $0.13^{+0.02}_{-0.01}$ keV in the source rest frame for RX J2241.8−4405 and PG 2233+134, respectively. Although the blackbody component is not statistically required, the fit for PG 1543+489 could yield the temperature of $0.16^{+0.07}_{-0.06}$ keV. For RX J1225.7+2055, the temperature was far from being constrained because of poor statistics. These obtained temperatures are again rather typical among NLS1s; e.g., $kT_{\rm diskpn}$ = 0.14–0.20 keV[2] (e.g., Leighly 1999, Porquet et al. 2004). We also tested a broken power-law model for the two sources with significant soft excess feature. For both cases, the obtained χ^2 values were slightly worse than those from the fit with the blackbody model with same degrees of freedom ($\Delta\chi^2 \sim 5$). The break energies in the observed frame were 1.0±0.2 keV and $1.6^{+1.0}_{-0.7}$ keV for RX J2241.8−4405 and PG 2233+134, respectively. The power-law indices below the break energy were 3.2±0.2 and 2.7±0.1 for RX J2241.8−4405 and PG 2233+134, respectively. With physical point of view a Comptonized blackbody model are considered more appropriate, but, we will not report such fits because limited quality of the data prevents us constrain parameters.

[2]The inner disk temperature of a multicolor blackbody model of diskpn in XSPEC. This value is larger by several times ten percent than that from the fit with a single temperature blackbody model.

3.2. UV–X-ray Spectral Slopes: α_{ox}

One of the great advantage of *XMM-Newton* for this research is that it can perform observation in UV and X-ray bands simultaneously. In order to obtain fluxes and spectral slopes in the UV band, we performed UV photometric observation by the OM with two filters for each object. The choice of filters are yielded by bright stars in the OM field of view; we used the U and UVM2 filters for PG 1543+489 and RX J1225.7+2055, and the UVW1 and UVW2 filters for the others. The effective wavelength of U, UVW1, UVM2, and UVW2 filters are 344, 291, 231, and 212 nm, respectively.

We utilized the pipeline products, and converted the OM counts rate into the fluxes using the method described at an *XMM-Newton* web page.[3] Then, attenuation by Galactic reddening is corrected using a reddening curve[4] and E(B−V) values taken from the NED.

We investigated UV–X-ray spectral slopes of our targets utilizing a parameter of α_{ox}, which is conventionally defined as a power-law energy index bridging two points of 2500 Å and 2 keV in the rest frame. The 2 keV fluxes can be directly measured by X-ray spectra, and the fluxes at 2500 Å are estimated by interpolating or extrapolating the observed OM fluxes with a power law. Unfortunately for PG 1543+489, no good data were obtained with U filter, hence we assumed that the spectral slope is the mean value of those from the other three sources.[5] The resulting α_{ox} values are also listed in Table 1.

Contrary the others showed rather normal $\alpha_{ox}\sim$1.5–1.6, RX J1225.7+2055 was found to be X-ray weak ($\alpha_{ox}\sim$2.0) during our observation (See also Figure 1). Thus, our observations show that not all NLQSOs are X-ray weak; at the same time, that not only PHL 1811 is anomalously X-ray weak.

[3]http://xmm.vilspa.esa.es/sas/documentation/watchout/uvflux.shtml
[4]http://idlastro.gsfc.nasa.gov/ftp/pro/astro/ccm_unred.pro
[5]The three spectral slopes range α_ν = 0.1–0.4, and we assumed the slope of PG 1543+489 is α_ν = 0.27. If we assume it is same as the slope from the SDSS composite (α_ν = 0.44; Vanden Berk et al. 2001), the resulting 2500 Åflux gets smaller by 7 %. The difference in the α_{ox} values is as small as $\Delta\alpha_{ox}$ = 0.01. Although it is reported that the average NLS1 UV spectrum shows rather red color ($\alpha_\nu \sim 0.8$), there is a trend relating α_ν and luminosity (Constantin & Shields, 2003). Among the luminous end of their sample, α_ν is about 0.5.

4. DISCUSSION

4.1. More Luminous, More Frequently X-ray Weak?

To investigate $\alpha_{\rm ox}$ distribution among luminous NLS1s in general, we compiled a heterogeneous sample of rather luminous AGNs ($M_{\rm v} < -23$) with narrow Hβ line from the literatures (White et al. 2000, Bade et al. 1998, Veron-Cetty & Veron 2001, among others). The 2500 Å flux (l_o) was estimated from optical magnitude taken from the references by extrapolating a power law of $f_\nu \propto \nu^{-0.44}$. The assumed spectral index of $\alpha_\nu = 0.44$ is based on that from the SDSS Quasar composite spectrum (Vanden Berk et al., 2001). The 2 keV fluxes were estimated from the count rates or upper limits obtained from RASS, assuming that the X-ray spectrum can be represented by Galactic absorbed power law with photon-index of 2.75 (Williams, Pogge, & Mathur 2002; Williams, Mathur, & Pogge 2004). The resulting values of $\alpha_{\rm ox}$ are plotted as a function of monochromatic luminosity at 2500 Å in Figure 1.

With above analysis, We discovered four additional X-ray weak objects in relatively luminous regime ($\log l_o > 30.6$). If we make statistics of X-ray weak objects in the several luminosity range, for example, $\log(l_o)$ below and above 30.3, only 2 among 18 objects are X-ray weak in the lower luminosity regime, whilst 6 among 17 objects show X-ray weakness in the higher. Although it is not statistically clear, it is suggested that X-ray weak objects might be found more frequently in more luminous regime.

It should be noted that no "X-ray bright" source was found. Variability with large-amplitude is common nature of NLS1s, but, if X-ray weakness is just because of fluctuation of flux around the average flux, we should find "X-ray bright" objects as frequently as X-ray weak ones. Contrary, Figure 1 shows that no source exhibits X-ray brightness with $\Delta\,\alpha_{\rm ox} \gtrsim 0.5$. Thus, X-ray weakness is not just caused by such fluctuation, instead some mechanism is likely to exist to make sources selectively fainter in the X-ray band.

It is true that NLS1s show skewed variability pattern in their light curves, and that they are characterized by flare-like peaked patterns (e.g., McHardy et al. 2004). For such a light curve, the time-averaged flux level is located at the level much lower than the median value. Then, we expect X-ray bright sources at less frequency and with larger amplitude, and X-ray faint sources at more frequency and with less amplitude. At least, from the point of frequency, this trend does not conflict with Figure 1; however, we cannot discuss with respect to the amplitude, because Figure 1 lacks X-ray bright sources. Thus we cannot rule out this explanation completely, but this predicts that the overall amplitude of variability (taking into account the not-yet-observed X-ray bright phase) is as large as several orders of magnitude, which has not been reported so far.

4.2. X-ray Weakness in Low-State of Transients?

In our *XMM-Newton* observation RX J1225.7+2055 was X-ray weak; however, during RASS it was 30 times brighter with normal $\alpha_{\rm ox}$. Another X-ray weak object found in our study with larger sample (H1137−127) was also found to have similar large-amplitude long-term variability: It was detected by *HEAO-1* survey with the 2–10 keV luminosity of $\log L_{\rm X} = 46.29$ erg s^{-1} (Remillard et al., 1993), and the RASS count rate predicts the luminosity fainter by 2 orders of magnitude. These facts mean that the some X-ray weak objects are not always to be so, and that they are in a transient state.

As Uttley et al. (2004) show in a NLS1 NGC 4051, hard X-ray spectra of AGN in general tend to be flatter when they are in fainter-state. Unfortunately because the net exposure time of RX J1225.7+2055 was significantly reduced because of background flare, we cannot investigate its power-law index solely in the hard X-ray band. In order to look at this property and also possible time short-variability, further and longer observations are necesarry for RX J1225.7+2055.

4.3. Physical Driver of X-ray Weakness

Attenuation by absorber is a way to explain observed X-ray weakness; in fact, We can not rule out this possibility for the other X-ray weak objects estimated by RASS. For RX J1225.7+2055, however, attenuation by absorption is unlikely to be the case because of its steep spectra, and because it was previously observed with "X-ray normal" during RASS. Of course, we cannot rule out completely this possibility, if Compton-thick cold absorption appeared in the our line-of-sight between the RASS and *XMM-Newton* observations separated by 10 years.

Intrinsic X-ray weakness could be more likely. As described in §1, another optically-luminous NLQSO, PHL 1811, is now securely confirmed to be intrinsically X-ray weak (Leighly et al. 2004; Leighly et al. in prep.). Since we selected the sample with relatively narrow Hβ line width, the luminosity axis is considered to be strongly correlated with accretion rate. The observed trend that more X-ray weak objects are found in more luminous regime implies that X-ray weakness is a nature of high $L/L_{\rm Edd}$, though they are not always so.

4.4. Implications from a disk-corona model

What is the implications of the X-ray weakness in terms of accretion disk models? Here, we try to interpret the $\alpha_{\rm ox}$ v.s. l_o diagram, based on simple disk models of an accretion disk sandwiched by coronae. The energy dissipation rate at the corona normalized to the total (corona plus disk) dissipated energy (often noted as f) can be estimated by considering either gas evaporation rate from the disk (Meyer & Meyer-Hofmeister 1994), or energy

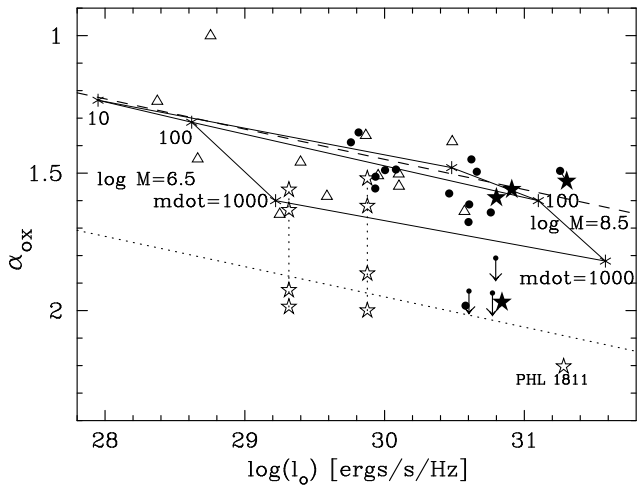

Figure 1. $\alpha_{\rm ox}$ *of NLS1s as a function of monochromatic luminosity at 2500 Å from our* XMM-Newton *observations (filled stars) along with those from heterogeneous samples. Filled circles are newly investigated data, using the* ROSAT *all-sky survey (RASS) X-ray fluxes and the optical fluxes in NED database. For the objects which could not be detected in RASS, 3*σ *upper-limits of* $\alpha_{\rm ox}$ *are shown with arrows. Data marked with open triangles and stars are taken from Leighly (2001b). The dashed line represents the regression among radio quiet quasars (Vignali et al. 2003), and the dotted line is parallel to the dashed done (*$\Delta\,\alpha_{\rm ox} = 0.5$*; the sources at the dotted line have are 20 times X-ray weaker than the sources at the dashed line), and is shown to guide the eye. The results calculated from the disk-corona model are shown with asterisks. Here we show the results in the cases of* $M_{\rm BH} = 10^{6.5}$ *and* $10^{8.5}$ *solar mass, and the accretion rate of* $\dot{m} = 10, 100, 1000$.

leakage due to magnetic buoyancy from the disk. For instance, Janiuk & Czerny (2000) showed that f, in the framework of an evaporating disk model, decreases when an gas accretion rate $\dot{M}$ increases (see also Bechtold et al. 2003, their Fig. 7). Similarly, Merloni & Fabian (2002) presented, with magnetic coronal models, a decreasing f for an increasing $\dot{m}$ [where $\dot{m} \equiv \dot{M}/(L_{\rm Edd}/c^2)$].

It is out of the scope of this paper to judge and discriminate various coronal models, and we simply adopt the prescription by Merloni & Fabian (2002):[6] Based on their Fig. 1, the ratio of the coronal power-law X-ray luminosity to the total bolometric one is assumed to be proportional to $\dot{m}^{-0.4} M_{\rm BH}^{-0.06}$. The X-ray luminosity is normalized so that the disk-corona model is consistent with the observed $\alpha_{\rm ox}$ of Ton S 180 (Turner et al. 2002) and PG 1448 (Kawaguchi et al. in prep.), [7] and the X-ray power-law index Γ is assumed to be a constant. Optical and bomoletric luminosities for various $\dot{m}$ and $M_{\rm BH}$ are taken from disk models of Kawaguchi (2003) with a constant viscosity parameter α of 0.01. The results are shown in Figure 1.

Firstly, Figure 1 shows that the slope of the regression line by Vignali et al. 2003 ($d\alpha_{\rm ox}/d\log l_o \approx -0.1$) can be explained by changing $M_{\rm BH}$ with a fixed $\dot{m}$. Given a larger $M_{\rm BH}$, an accretion disk becomes cooler, shining at longer wavelength (optical) with smaller $\alpha_{\rm ox}$. On the other hand, a smaller $M_{\rm BH}$ tends to make the disk shine at shorter wavelength (e.g., UV), and hence with larger $\alpha_{\rm ox}$. In other words, accretion disk models predict that bolometric luminosities are not necessarily in proportion to optical luminosities, as emphasized in Hosokawa et al. (2000, §2.3.1). Actually, Collin & Kawaguchi (2004) showed, by using the data of X-ray selected AGNs obtained by Grupe et al. (2004), that optical luminosities roughly scale as $L_{\rm bol}^{0.7}$.

Secondly, the deviation of $\alpha_{\rm ox}$ from the regression relation seems to be controlled by $\dot{m}$. This disk-corona model turns out to cover the distribution of most of the plotted objects (except for the X-ray weak ones, as discussed below). A large offset of $\alpha_{\rm ox}$ happens when $\dot{m}$ changes from 100 to 1000, where the bolometric luminosity increases very little due to saturation of disk emission by photon trapping (Abramowicz et al. 1988; Begelman 1978), while the optical luminosity continues to increase since the outer region of the disk, responsible for optical emission, is still outside the photon trapped region (see Kawaguchi 2003). Observational data seem to support this trend. Wang, Watarai & Mineshige (2004) pointed out that the ratio of X-ray (2–10 keV) luminosity over optical luminosity is anticorrelated with the ratio of optical luminosity over Eddington luminosity. (Note, however, that the anticorrelation is trivial if the 2–10 keV luminosity is roughly in proportion to the BH mass.)

Finally, it is now clear that the X-ray weak objects are located outside the region predicted by this simple disk-corona model. The X-ray weakness could be originated in either (i) an extremely large $\dot{m}$ (> 1000), or (ii) an extremely low energy dissipation rate at the corona, f (by some unknown physical mechanisms). Let us go back again to the case of PHL 1811. Its Hβ width and optical luminosity imply (Kaspi et al. 2000; Wandel et al. 1999) that its BH mass is around $10^{8.5}$ to $10^9 M_\odot$. Based on the spectral model in Kawaguchi (2003, Fig. 11), the optical luminosity and inferred BH mass indicate $\dot{m}$ to be between 100 and 1000. Therefore, at least for this object, the hypothesis (i) with an extremely large $\dot{m}$ (> 1000) is not likely. Although the second interpretation (ii) is favored, the physical reason behind very low f is still unclear. Frequency of the X-ray weakness (this study), a search for common properties of X-ray weak objects, and detailed observations of the X-ray weak objects who transient between X-ray weak and X-ray normal regimes will help to understand what is going on there. Theoret-

[6] Their model is in principle limited to sub-Eddington accretion rate ($\dot{m} \leq 16$). However, the $M_{\rm BH}$-dependency of f found for sub-Eddington rates are likely valid also for super-Eddington rates, since the $M_{\rm BH}$-dependency of physical quantities in super-Eddington disks is identical to that of the standard disk (e.g., Fukue 2000).

[7] Their $M_{\rm BH}$ and $\dot{m}$ are estimated to be $\sim 10^{6.5-7} M_\odot$ and ~ 1000, respectively (Kawaguchi, Pierens, & Huré, 2004; Kawaguchi 2004).

ical investigations on a corona above a super-Eddington accretion disk are also insufficient.

ACKNOWLEDGMENTS

This work is based on observations obtained with *XMM-Newton*, an ESA science mission with instruments and contributions directly funded by ESA Member States and NASA. We acknowledge the great efforts of all the members of the *XMM-Newton* team. This research has made use of the NASA/IPAC Extragalactic Database (NED) which is operated by the Jet Propulsion Laboratory, California Institute of Technology, under contract with the National Aeronautics and Space Administration. CM gratefully acknowledges support through the Grant-in-Aid for Scientific Research (17740104) of the Ministry of Education, Culture, Sports, Science and Technology.

REFERENCES

Bade, N. et al. 1998, A&AS, 127, 145

Abramowicz, M. A., Czerny, B., Lasota, J. P., & Szuszkiewicz, E. 1988, ApJ, 332, 646

Begelman, M. C. 1978, MNRAS,184, 53

Bechtold, J. et al. 2003, ApJ, 588, 119

Boller, Th., Brandt, W. N., & Fink, H. 1996, A&A, 305, 53

Brandt, W. N., Mathur, S., & Elvis, M. 1997, MNRAS, 285, L25

Collin & Kawaguchi 2004, A&A, 426, 797

Constantin, A. & Shields, J. C. 2003, ApJ, 115, 592

Fukue, J. 2000, PASJ, 52, 829

Goodrich, R. W. 1989, ApJ, 342, 224

Ghisellini, G., Haardt, & F., Matt, G. 1994, MNRAS, 267, 743

Hosokawa, T., Mineshige, S., Kawaguchi, T., Yoshikawa, K., & Umemura, M. 2001, PASJ, 53, 861

Janiuk, A., & Czerny, B. 2000, NewAR, 5, 7

Kaspi, S., Smith, P. S., Netzer, H., Maoz, D., Jannuzi, B. T., & Giveon, U. 2000, ApJ, 533, 631

Kawaguchi, T., Pierens, A., & Huré, J.-M. 2004, A&A, 415, 47

Kawaguchi, T. 2004, Prog. Theor. Phys. Suppl., 155, 120

Grupe, D., Wills, B. J., Leighly, K. M., Meusinger, H. 2004, AJ, 127, 156

Laor, A. 2000, NewAR, 44, 503

Leighly, K. M. 1999, ApJS, 125, 317

Leighly, K. M., Halpern, J. P., Helfand, D. J., Becker, R. H., & Impey, C. D. 2001a, AJ, 121, 2889

Leighly, K. M. 2001b, Proceeding of "X-ray Emission from Accretion onto Black Holes" ADS Bibliographic Code: 2001xeab.confE..38L

Leighly, K. M., Halpern, J. P., & Jenkins E. B. 2004, in "AGN Physics with the Sloan Digital Sky Survey", eds. G. T. Richards & P. B. Hall, ASP, in press

McHardy, I. M., Papadakis, I. E., Uttley, P., Page, M. J., Mason, K. O. 2004, MNRAS, 348, 783

Merloni, A. & Fabian, A. C. 2002, MNRAS, 332,165

Meyer, F., & Meyer-Hofmeister, E. 1994, A&A, 288, 175

Osterbrock, D. E., & Pogge, R. W. 1985, ApJ, 297, 166

Porquet, D., Reeves, J. N., O'Bruien, P., &, Brinkmann, W. 2004, A&A, 422, 85

Pounds, K. A., Done, C., & Osborne, J. P. 1995, MNRAS, 277, L5

Remillard, R. A., Bradt, H. V. D., Brissenden, R. J. V., Buckley, D. A. H., Roberts, W., Schwartz, D. A., Stroozas, B. A., & Tuohy, I. R. 1993, AJ, 105, 2079

Turner, T. J. et al. 2002, ApJ, 568, 120

Uttley, P., Taylor, R. D., McHardy, I. M., Page, M. J., Mason, K. O., Lamer, G., Fruscione, A. 2004, MNRAS, 347, 1345

Vanden Berk, D. E. et al. 2001, AJ, 122, 549

Veron-Cetty M. P. & Veron P. 2001, A&A, 374, 92

Vignali, C., Brandt, W. N., Schneider, D. P. 2003, AJ, 125, 433

Voges, W. et al. 1999, A&A, 349, 389

Wandel, A., Peterson, B. M., & Malkan, M. A. 1999, ApJ, 526, 579

Wang, J., Watarai, K. & Mineshige, S. 2004, ApJ, 607, L107

White, R. L. et al. 2000, ApJS, 126, 133

Williams, R., Pogge, R. W., & Mathur, S. 2002, AJ, 124, 3042

Williams, R., Mathur, S. & Pogge, R. W. 2004, ApJ, 610, 737